considerably. While AD-PHA1 shows a gradual clinical improvement with advancing age, usually allowing the cessation of salt supplementation during infancy, AR-PHA1 persists into adulthood, and no improvement is typically seen with time [1, 2]. Here, we report a patient with AR-PHA1 who demonstrated an improvement of clinical severity, leading to the cessation of salt supplementation. To clarify the mechanism behind this phenomenon, we assessed the segmental sodium-reabsorption ability of the patient and compared it to that of an AD-PHA1 patient. In addition, quantification of the levels of thiazide-sensitive Na^+-Cl^- cotransporter (NCC) protein in their urine samples was also performed.

Patient reports

Patient with AR-PHA1 (patient 1)

This patient, who is currently 20 years old, is a compound heterozygote with a documented mutation in the ENaC γ-subunit (γENaC) gene (1627delG and 1570-1G → A), and a case report that outlined his situation until 7 years of age was previously produced [3]. In brief, he collapsed at 7 days of age with marked hyponatremia (116 mEq/L) and hyperkalemia (8.6 mEq/L). Findings of a raised plasma aldosterone level and an adequate cortisol response led to the diagnosis of PHA1. Despite heavy salt supplementation (up to 6 g a day), he repeatedly experienced salt-wasting episodes during his childhood and needed frequent hospitalization. With advancing age, however, he experienced fewer episodes of salt depletion or hospitalization. At age 11, salt supplementation was stopped. He is now 157.9 cm tall (−2.2 SD for a Japanese male) and is working as a factory worker. During the last 8 years, he has been hospitalized for salt wasting only once, and has received intravenous therapy as an outpatient only thrice. His latest laboratory data were as follows: serum Na 131 mEq/L, K 5.5 mEq/L, plasma aldosterone 15,000 pg/mL (normal range for corresponding age: 15.6–398).

Patient with AD-PHA1 (patient 2)

This patient has a heterozygous NR3C2 gene mutation (L924P), as reported previously (patient II-2 of our previous report [4]). Briefly, he was hospitalized for poor weight gain at the age of 7 days. His low sodium level (132 mEq/L) and elevated plasma aldosterone suggested PHA1. He was treated with salt supplementation (1.5 g a day) until 11 months of age. Thereafter, he experienced no salt wasting episodes despite the absence of maintenance therapy. He is now 19 years old and attending college. His latest laboratory data were as follows: serum Na 139 mEq/L, K 4.1 mEq/L, plasma aldosterone 440 pg/mL.

Methods

Measurement of segmental tubular reabsorption

According to the method described by Bartoli and Romano [5], the amount of sodium reabsorption in the distal nephron (including the distal convoluted tubule, connecting segment, and collecting duct) was estimated under maximal water diuretic conditions in both PHA1 patients. After overnight fasting, each subject was instructed to drink 20 mL/kg of water over 30 min. Simultaneously, the intravenous infusion of half normal saline was started at a rate of 1,000 mL/h/1.73 m^2. After 3 h, when the achievement of maximum water diuresis was ascertained by a urine osmolarity of less than 50 mOsm/L, furosemide 1 mg/kg was injected intravenously, while the infusion rate of half normal saline was raised to 1,500 mL/h/1.73 m^2. During this period, blood sampling was carried out every 20 min via an indwelling catheter inserted in the contralateral antecubital vein. Urine samples were also collected between each blood sampling by spontaneous voiding. The patients were instructed not to interrupt voiding but to excrete urine completely, in order to avoid bladder catheterization.

Osmolarity (Uosm and Posm, respectively) and creatinine concentration (Ucr and Pcr, respectively) were measured in every urine and plasma sample by the in-house laboratory. Free water clearance (C_{H_2O}) was defined as the difference between urine volume (V) and osmolar clearance (Cosm) [$C_{H_2O} = V -$ Cosm]. Then, the C_{H_2O} after furosemide infusion (fC_{H_2O}) was considered to reflect the amount of sodium reabsorption generated by the distal nephron (C_{H_2O-DT}). The amount of sodium reabsorption generated by the loop of Henle (C_{H_2O-HL}) was estimated by the difference between the osmolar clearance during maximal diuresis and that following furosemide infusion [$C_{H_2O-HL} = fCosm -$ Cosm.]

Detection of the NCC protein in urine

According to the methods described by Pisitkun et al. [6] and Zhou et al. [7], immunoblotting of the NCC protein in urine samples was performed in the two patients, as well as in age- and sex-matched normal controls, as described below.

The isolation of urinary proteins in the exosome fraction

All the steps mentioned below were performed at 4°C. Immediately after urine collection, one protease inhibitor

cocktail tablet (Complete®: Roche Diagnostics, Mannheim, Germany) was added per 50 mL of urine to avoid proteolysis, and urine samples were centrifuged at 1,500×g for 10 min. The supernatant was centrifuged using a HITACHI himac CR21 (Hitachi Koki Co., Ltd, Tokyo, Japan) at 17,000×g for 15 min to remove whole cells, large membrane fragments, and debris. Then, the supernatant was centrifuged with a HITACHI himac CP100α ultracentrifuge (Hitachi Koki Co., Ltd) at 200,000×g for 1 h. After removal of the supernatant, the pellets were suspended in 25 μL isolation solution consisting of 10 mM triethanolamine and 250 mM sucrose (pH 7.6). The suspension was then added to an equal volume of 2× sample buffer [50 mM Tris–HCl (pH 6.8), 10% glycerol, 2% SDS, and bromophenol blue]. These samples were heated at 90°C for 5 min and then stored at −80°C until use. It is now recognized that this fraction of urine is largely made up of excreted exosomes [6].

Gel electrophoresis and immunoblotting

Ten microliters of each urine sample were subjected to SDS-PAGE with 4–20% polyacrylamide slab gels (e-PAGEL®, ATTO Corporation, Tokyo, Japan). The electric transfer onto a polyvinylidene difluoride membrane was carried out with a semidry blotting apparatus (Bio-Rad Laboratories, Bio-Rad Japan, Tokyo) at 15 V for 30 min at room temperature using buffer containing three kinds of solutions (A: 300 mM Tris/5% methanol, B: 25 mM Tris/5% methanol, C: 25 mM Tris/6-amino capronic acid/5% methanol). After being blocked with 5% milk in 20 mM Tris–HCl buffer (pH 7.5) containing 150 mM NaCl for 1 h, the membranes were probed with antibodies: polyclonal antibodies to NCC and the Na^+–K^+–Cl^- cotransporter (NKCC2) dissolved 1/200 in Can Get Signal (TOYOBO Co. Ltd., Tokyo, Japan) were used for 1 h at room temperature. Horseradish peroxidase: HRP-conjugated, goat anti-rabbit IgG (Santa Cruz Biotechnology, Inc., Santa Cruz, CA, USA) dissolved 1/10,000 in Can Get Signal was used for 1 h at room temperature. The antibody–antigen reaction procedure was performed using the SuperSignal West Pico Chemiluminescent Substrate (Pierce, Thermo Fisher Scientific K.K., Yokohama, Japan). The density of the 164 kDa band, which corresponded to NCC, was quantified by densitometry (Quantity One software, Bio-Rad Laboratories), and then the densities were corrected for both creatinine concentration and the NKCC2 densities in the urine sample.

Informed consent to participate in the above studies was obtained from both the patients and their parents. The study protocols were approved by the institutional review board of Kanagawa Children's Medical Center, and the study was carried out according to the principles of the Declaration of Helsinki.

Results

The results of the segmental tubular function analysis are shown in Table 1. C_{H_2O-DT} (free water clearance by the distal nephron, indicating sodium reabsorption by the distal nephron) was decreased in both PHA1 patients, which is consistent with impaired sodium reabsorption at the distal nephron, downstream from the loop of Henle. The value, however, was almost identical in both patients, despite their different genetic etiologies. In addition, PD (proximal delivery), the flow escaping proximal reabsorption, was decreased in both patients compared with appropriate reference values.

Figure 1 shows immunoblotting of the NCC protein in urine samples performed on two separate occasions. In both experiments, patient 1 showed the highest concentration of NCC, which was expressed as density per creatinine, with significant statistical differences between the mean value in patient 1 and those of seven controls ($P < 0.01$, unpaired t test). When expressed as NCC density per NKCC2 density, the highest value was also found in patient 1 (4.25), compared with the mean value of the normal controls (0.99).

Discussion

Clinical improvement in AD-PHA1 is a well-recognized phenomenon [1, 2], although the reason for it is not yet fully understood. Patient 1 may be the first example of clinical improvement in a molecularly proven AR-PHA1, because he has been free from salt supplementation without clinical deterioration since 11 years of age. To elucidate the mechanism behind this phenomenon, we concentrated on the differences in the expression sites of ENaC and MR in the distal nephron. Whereas ENaC is expressed along the entire collecting duct (CD) and connecting tubule (CNT), the MR is also present in the distal convoluted tubule

Table 1 Results of maximal water diuresis data in AR- and AD-PHA1 patients

	V	C_{H_2O}	C_{H_2O-HL}	C_{H_2O-DT}	PD
Patient 1 (AR-PHA1)	8.4	6.22	12.8	2.48	17.4
Patient 2 (AD-PHA1)	11.6	8.49	13.9	2.98	20.0
Reference	18 ± 1	13 ± 1	17 ± 1	9 ± 1	31 ± 1

AR-PHA1, autosomal recessive form of pseudohypoaldosteronism type 1; AD-PHA1, autosomal dominant form of pseudohypoaldosteronism type 1; V, urine flow rate; C_{H_2O}, free water clearance excreted; C_{H_2O-HL}, free water formed by Henle's loop; C_{H_2O-DT}, free water formed by the distal nephron; PD, proximal delivery. Each figure is expressed as milliliters per minute per 100 mL of GFR (mL/min/dLGFR). For details, see the "Methods" section of the text. The reference values were taken from [5]
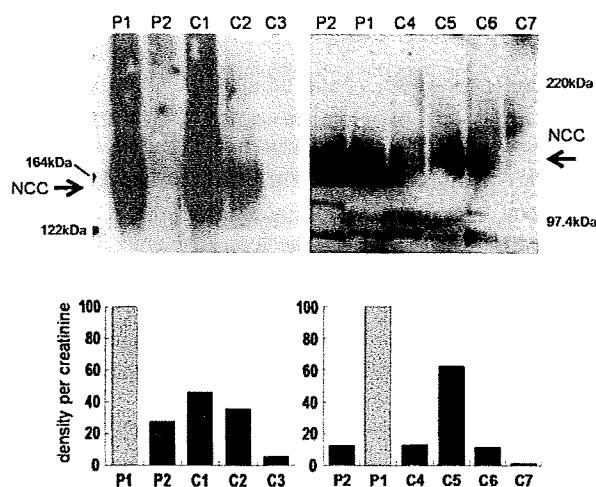
Fig. 1 Results of NCC immunoblotting in urine samples from AR- and AD-PHA1 patients and age- and sex- matched normal controls conducted on two separate occasions. The *upper panel* shows the electrophoresis patterns. *P1*, patient 1; *P2*, patient 2; *C1–C7*, control samples. In the *lower panel*, quantitative data obtained from a densitometer (corrected for creatinine) is shown. Note that each result is expressed as the ratio to that of patient 1, which was set to 100

(DCT), in which NCC is also expressed. In addition, it has also been demonstrated that the expression of NCC is upregulated by aldosterone [8]. Therefore, we hypothesized that, in patient 1, increased expression of NCC under aldosterone hypersecretion may compensate for defective ENaC function.

Segmental tubular functional analysis under maximal water diuresis [5] showed that the sodium reabsorption from the distal nephron (deduced from the C_{H_2O-DT} data) was almost identical in the AR- and AD-PHA1 patients. This result seems discordant with the clinical severity of these patients, especially during infancy: patient 1 (AR-PHA1) suffered from repetitive salt-wasting episodes, whereas patient 2 (AD-PHA1) showed a less severe course. Rather, this finding supports our hypothesis that increased NCC expression compensated for the lack of ENaC sodium reabsorption in the distal nephron in patient 1.

Since the direct demonstration of NCC abundance is difficult in human studies, we performed immunoblotting of the NCC protein using urine samples. In rats, it has been shown that the urinary levels of tubular sodium transporters closely reflect their abundance in the kidney [9]. As data from human samples are scarce, our data need further investigation. However, the increased NCC level in patient 1, irrespective of the denominator used (creatinine or NKCC2 density), seems consistent with our hypothesis.

The compensatory hyperfunction of NCC is not surprising, since it has been demonstrated that NCC abundance is upregulated under sodium restriction and/or aldosterone infusion in the rat kidney [9]. In addition, the

expression of NHE3 (type 3 Na/H exchanger) in the proximal tubule is known to increase under long-term acid loading in rats [10]. Furthermore, the up-regulation of ENaC has also been demonstrated in rats [11]. Although the mechanisms behind such compensatory pathways have not been fully elucidated, it has been speculated that aldosterone upregulates NCC not by transcriptional regulation, but by effects on translation or protein half-life [12].

In this context, the decreased PD (proximal delivery: the flow escaping proximal reabsorption) observed in both PHA1 patients was interesting. A decreased PD indicates that a lower amount of urine is arriving at the distal nephron. It may be the case that NHE3 or other sodium channels in proximal tubules also compensate for sodium reabsorption. An alternative explanation is that it reflects tubuloglomerular feedback, the process by which the kidney regulates glomerular filtration in response to altered tubular flow.

It seems reasonable to suggest that NCC upregulation also occurs in other AR-PHA1 patients. However, severe salt wasting is not ameliorated in most AR-PHA1 patients. Accordingly, mechanism(s) other than NCC hyperfunction may have ameliorated the salt wasting seen in patient 1. First, the presence of an intact ENaC α subunit (αENaC) may play a role. ENaC is made up of three homologous subunits (α, β, and γ), which probably have a stoichiometry of 1:1:1 [13–15]. Of these, αENaC plays a central role in channel function, whereas residual activity can be measured in the absence of β or γ subunits [13]. Recent studies have suggested that channels with alternative stoichiometry (such as α, αγ, or αβ channels) can function at the cell membrane, albeit with substantially lower activity compared to the native αβγ channel [15, 16]. Thus, the activity of ENaC that does not contain the γ subunit may have partly contributed to the amelioration of the clinical severity seen in patient 1. In contrast, this mechanism will not work in AR-PHA1 cases involving αENaC deficiency, which correspond to about two-thirds of the hitherto reported AR-PHA1 cases [1, 2]. A second possibility is that the γENaC in patient 1 retained some residual channel activity. In fact, a case that demonstrated a mild clinical manifestation (onset at 19 days of age) due to a G37S βENaC mutation causing an estimated channel activity of 40% has been reported [17]. The validity of this hypothesis in patient 1 must be subjected to further study because no expression study evaluating mutated channel function has been carried out. However, we think that this scenario is unlikely because both mutations abolish γENaC transmembrane domain 2 and lead to the complete loss of its function.

Finally, because the urinary NCC level in patient 2 was not different from that of the controls, the clinical improvement in AD-PHA1 does not seem to be related to

NCC upregulation. This further indicates that aldosterone can upregulate NCC only via MR.

In conclusion, we observed an amelioration of clinical severity in an AR-PHA1 patient due to γENaC mutations. An increased number of NCC may have been responsible, at least in part, for this phenomenon.

References

1. Geller DS. Mineralocorticoid resistance. Clin Endocrinol (Oxf). 2005;62:513–20.
2. Zennaro MC, Lombès M. Mineralocorticoid resistance. Trends Endocrinol Metab. 2004;15:264–70.
3. Adachi M, Tachibana K, Asakura Y, Abe S, Nakae J, Tajima T, et al. Compound heterozygous mutations in the gamma subunit gene of ENaC (1627delG and 1570-1G → A) in one sporadic Japanese patient with a systemic form of pseudohypoaldosteronism type 1. J Clin Endocrinol Metab. 2001;86:9–12.
4. Tajima T, Kitagawa H, Yokoya S, Tachibana K, Adachi M, Nakae J, et al. A novel missense mutation of mineralocorticoid receptor gene in one Japanese family with a renal form of pseudohypoaldosteronism type 1. J Clin Endocrinol Metab. 2000;85:4690–4.
5. Bartoli E, Romano G. Measurement of reabsorption by single segments of the human nephron. J Nephrol. 1999;12:275–87.
6. Pisitkun T, Shen RF, Knepper MA. Identification and proteomic profiling of exosomes in human urine. Proc Natl Acad Sci USA. 2004;101:13368–73.
7. Zhou H, Yuen PS, Pisitkun T, Gonzales PA, Yasuda H, Dear JW, et al. Collection, storage, preservation, and normalization of human urinary exosomes for biomarker discovery. Kidney Int. 2006;69:1471–6.
8. Kim GH, Masilamani S, Turner R, Mitchell C, Wade JB, Knepper MA. The thiazide-sensitive Na–Cl cotransporter is an aldosterone-induced protein. Proc Natl Acad Sci USA. 1998;95:14552–7.
9. Knepper MA, Kim GH, Masilamani S. Renal tubule sodium transporter abundance profiling in rat kidney: response to aldosterone and variations in NaCl intake. Ann N Y Acad Sci. 2003;986:562–9.
10. Kim GH, Martin SW, Fernández-Llama P, Masilamani S, Packer RK, Knepper MA. Long-term regulation of renal Na-dependent cotransporters and ENaC: response to altered acid-base intake. Am J Physiol Renal Physiol. 2000;279:F459–67.
11. Frindt G, Palmer LG. Na channels in the rat connecting tubule. Am J Physiol Renal Physiol. 2004;286:F669–74.
12. Masilamani S, Wang X, Kim GH, Brooks H, Nielsen J, Nielsen S, et al. Time course of renal Na-K-ATPase, NHE3, NKCC2, NCC, and ENaC abundance changes with dietary NaCl restriction. Am J Physiol Renal Physiol. 2002;283:F648–57.
13. Canessa CM, Schild L, Buell G, Thorens B, Gautschi I, Horisberger JD, et al. Amiloride-sensitive epithelial Na^+ channel is made of three homologous subunits. Nature. 1994;367:463–7.
14. Jasti J, Furukawa H, Gonzales EB, Gouaux E. Structure of acid-sensing ion channel 1 at 1.9Å resolution and low pH. Nature. 2007;449:316–23.
15. Butterworth MB, Weisz OA, Johnson JP. Some assembly required: putting the epithelial sodium channel together. J Biol Chem. 2008;283:35305–9.
16. Harris M, Garcia-Caballero A, Stutts MJ, Firsov D, Rossier BC. Preferential assembly of epithelial sodium channel (ENaC) subunits in *Xenopus* oocytes: role of furin-mediated endogenous proteolysis. J Biol Chem. 2008;283:7455–63.
17. Chang SS, Grunder S, Hanukoglu A, Rösler A, Mathew PM, Hanukoglu I, et al. Mutations in subunits of the epithelial sodium channel cause salt wasting with hyperkalaemic acidosis, pseudohypoaldosteronism type 1. Nat Genet. 1996;12:248–53.

Heterozygous Orthodenticle Homeobox 2 Mutations Are Associated with Variable Pituitary Phenotype

Sumito Dateki, Kitaro Kosaka, Kosei Hasegawa, Hiroyuki Tanaka, Noriyuki Azuma, Susumu Yokoya, Koji Muroya, Masanori Adachi, Toshihiro Tajima, Katsuaki Motomura, Eiichi Kinoshita, Hiroyuki Moriuchi, Naoko Sato, Maki Fukami, and Tsutomu Ogata

Department of Endocrinology and Metabolism (S.D., N.S., M.F., T.O.), National Research Institute for Child Health and Development, and Division of Ophthalmology (N.A.) and Department of Medical Subspecialties (S.Y.), National Children's Medical Center, Tokyo 157-8535, Japan; Department of Pediatrics (S.D., K.M., E.K., H.M.), Nagasaki University Graduate School of Biomedical Sciences, Nagasaki 852-8501, Japan; Department of Pediatrics (K.K.), Kyoto Prefectural University of Medicine, Graduate School of Medical Science, Kyoto 602-8566, Japan; Department of Pediatrics (K.H., H.T.), Okayama University Graduate School of Medicine, Dentistry, and Pharmaceutical Sciences, Okayama 700-8558, Japan; Division of Endocrinology and Metabolism (K.M., M.A.), Kanagawa Children's Medical Center, Yokohama 232-8555, Japan; and Department of Pediatrics (T.T.), Hokkaido University School of Medicine, Sapporo 060-8638, Japan

Context: Although recent studies have suggested a positive role of *OTX2* in pituitary as well as ocular development and function, detailed pituitary phenotypes in *OTX2* mutations and *OTX2* target genes for pituitary function other than *HESX1* and *POU1F1* remain to be determined.

Objective: We aimed to examine such unresolved issues.

Subjects: We studied 94 Japanese patients with various ocular or pituitary abnormalities.

Results: We identified heterozygous p.K74fsX103 in case 1, p.A72fsX86 in case 2, p.G188X in two unrelated cases (3 and 4), and a 2,860,561-bp microdeletion involving *OTX2* in case 5. Clinical studies revealed isolated GH deficiency in cases 1 and 5; combined pituitary hormone deficiency in case 3; abnormal pituitary structures in cases 1, 3, and 5; and apparently normal pituitary function in cases 2 and 4, together with ocular anomalies in cases 1–5. The wild-type Orthodenticle homeobox 2 (OTX2) protein transactivated the *GNRH1* promoter as well as the *HESX1*, *POU1F1*, and *IRBP* (interstitial retinoid-binding protein) promoters, whereas the p.K74fsX103-OTX2 and p.A72fsX86-OTX2 proteins had no transactivation functions and the p.G188X-OTX2 protein had reduced (~50%) transactivation functions for the four promoters, with no dominant-negative effect. cDNA screening identified positive *OTX2* expression in the hypothalamus.

Conclusions: The results imply that *OTX2* mutations are associated with variable pituitary phenotype, with no genotype-phenotype correlations, and that *OTX2* can transactivate *GNRH1* as well as *HESX1* and *POU1F1*. (*J Clin Endocrinol Metab* **95:** 756–764, 2010)

Pituitary development and function depends on the spatially and temporally controlled expression of multiple transcription factor genes such as *POU1F1*, *HESX1*, *LHX3*, *LHX4*, *PROP1*, and *SOX3* (1, 2). Whereas mutations of some genes (*e.g. POU1F1*) result in a relatively characteristic pattern of pituitary hormone deficiency, those of other genes (*e.g. HESX1*) are associated with a wide range of pituitary phenotype including combined pi-

Abbreviations: CGH, Comparative genomic hybridization; CPHD, combined pituitary hormone deficiency; EPP, ectopic posterior pituitary; FISH, fluorescence *in situ* hybridization; HD, homeodomain; IGHD, isolated GH deficiency; IRBP, interstitial retinoid-binding protein; MLPA, multiplex ligation-dependent probe amplification; NMD, nonsense mediated mRNA decay; OTX2, orthodenticle homeobox 2; PH, pituitary hypoplasia; SOD, septooptic dysplasia; TD, transactivation domain.

tuitary hormone deficiency (CPHD), isolated GH deficiency (IGHD), and apparently normal phenotype. However, because mutations of these genes account for a relatively minor portion of patients with congenital hypopituitarism (2, 3), multiple genes would remain to be identified in congenital hypopituitarism.

Orthodenticle homeobox 2 (*OTX2*) is a transcription factor gene primarily involved in ocular development (4). It encodes a paired type homeodomain (HD) and a transactivation domain (TD) and produces two functionally similar splice variants, isoform-a (GenBank accession no. NM_21728.2) and isoform-b (NM_172337.1) with and without eight amino acids because of alternative splice acceptor sites at the boundary of intron 3 and exon 4 (5). To date, at least 10 pathological heterozygous *OTX2* mutations have been identified in patients with ocular malformations such as anophthalmia and/or microphthalmia (6, 7). Ocular phenotype is highly variable, ranging from anophthalmia to nearly normal eye development, even in patients from the same family. Furthermore, most patients also exhibit brain anomaly, seizure, and/or developmental delay.

Recent studies have indicated that *OTX2* is also involved in pituitary development and function. Dateki *et al.* (8) showed that *OTX2* is expressed in the pituitary and has a transactivation function for the promoters of *POU1F1* and *HESX1* as well as the promoter of *IRBP* (interstitial retinoid-binding protein) involved in ocular function and that a frameshift *OTX2* mutation identified in a patient with bilateral anophthalmia and partial IGHD barely retained the transactivation activities. Subsequently a missense *OTX2* mutation with a dominant-negative effect and a frameshift *OTX2* mutation with loss-of-function effect were identified in CPHD patients with and without ocular malformation (9, 10).

However, detailed pituitary phenotypes in *OTX2* mutation-positive patients as well as other possible *OTX2* target genes for pituitary development and function remain to be determined. Here we report five new patients with *OTX2* mutations and summarize clinical findings in *OTX2* mutation-positive patients. We also show that *OTX2* is expressed in the hypothalamus and has a transactivation function for the promoter of *GNRH1*.

Patients and Methods

Patients

We studied 94 Japanese patients consisting of: 1) 16 patients with ocular anomalies and pituitary dysfunctions accompanied by short stature (<−2 SD) (six with anophthalmia and/or microphthalmia and CPHD, five with anophthalmia and/or microphthalmia and IGHD, three with septooptic dysplasia (SOD)

and CPHD, and two with SOD and IGHD) (group 1); 2) 12 patients with ocular anomalies whose pituitary functions were not investigated (one with bilateral microphthalmia and short stature, one with bilateral optic nerve hypoplasia and short stature, and 10 with anophthalmia and/or microphthalmia and normal stature) (group 2); and 3) 66 patients with pituitary dysfunctions but without ocular anomalies (five with IGHD and 61 patients with CPHD) (group 3). No demonstrable mutation was identified for *HESX1* in patients with SOD, *GH1* and *HESX1* in patients with IGHD, and *POU1F*, *HESX1*, *LHX3*, *LHX4*, *PROP1*, and *SOX3* in patients with various types of CPHD (2). All the patients had normal karyotype.

Primers and probes

The primers and probes used in this study are shown in Supplemental Table 1, published as supplemental data on The Endocrine Society's Journals Online web site at http://jcem.endojournals.org.
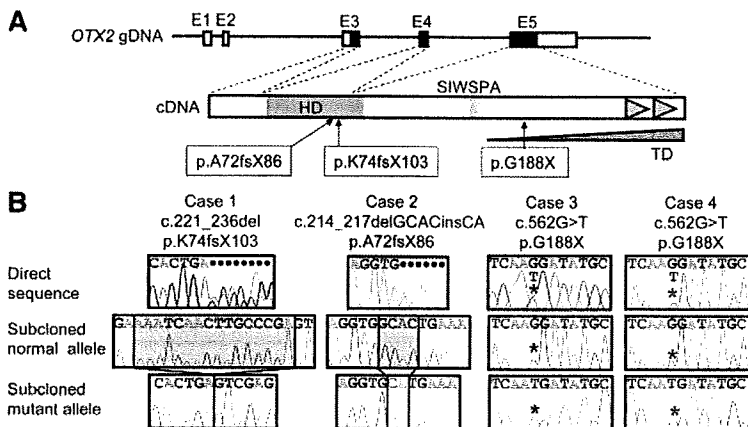
Sequence analysis of OTX2

This study was approved by the Institutional Review Board Committee at National Center for Child Health and Development. After obtaining written informed consent, the coding exons 3-5 and their flanking splice sites were PCR amplified using leukocyte genomic DNA samples of all 94 patients and were subjected to direct sequencing on a CEQ 8000 autosequencer (Beckman Coulter, Fullerton, CA). To confirm a heterozygous mutation, the corresponding PCR products were subcloned with TOPO TA cloning kit (Invitrogen, Carlsbad, CA), and normal and mutant alleles were sequenced separately.

Prediction of the occurrence of aberrant splicing and nonsense mediated mRNA decay (NMD)

To examine whether identified mutations could cause aberrant splicing by creating or disrupting exonic splicing enhancers and/or splice sites (11, 12), we performed *in silico* analyses with the ESE finder release 3.0 (http://rulai.cshl.edu/cgi-bin/tools/ESE3/esefinder.cgi) for the prediction of exonic splice enhancers and with the program at the Berkeley Drosophila Genome Project (http://www.fruitfly.org/seq_tools/splice.html) for the prediction of splice sites. We also analyzed whether identified mutations could be subject to NMD on the basis of the previous report (12, 13).

Deletion analysis

Multiplex ligation-dependent probe amplification (MLPA) was performed for *OTX2* intragenic mutation-negative patients as a screening of a possible microdeletion affecting *OTX2*. This procedure was performed according to the manufacturer's instructions (14), using probes designed specifically for *OTX2* exon 4 together with a commercially available MLPA probe mix (P236) (MRC-Holland, Amsterdam, The Netherlands) used as internal controls. To confirm a microdeletion, fluorescence *in situ* hybridization (FISH) was performed with a long PCR product for *OTX2* (a 6096 bp segment from intron 2 to exon 5) together with an RP11-566I2 BAC probe (14q11.2; Invitrogen, Carlsbad, CA) used as an internal control. The probe for *OTX2* was labeled with digoxigenin and detected by rhodamine anti-digoxigenin, and the control probe was labeled with biotin and

A

B

FIG. 1. Sequence analysis in cases 1–4. A, The structure of *OTX2* (the isoform-b) and the position of the mutations identified. The *black* and *white boxes* on genomic DNA (gDNA) denote the coding regions on exons 1-5 (E1-E5) and the untranslated regions, respectively. *OTX2* encodes the HD (a *blue region*), the SIWSPA conserved motif (an *orange region*), and the two tandem tail motifs (*green triangles*). The TD (a *gray triangle*) is assigned to the C-terminal side; deletion of each tail motif reduces the transactivation function, and that of a region distal to the SIWSPA motif further reduces the transactivation function. In addition, another TD may also reside in the 5′ side of the HD (17). The three mutations identified in this study are shown. B, Electrochromatograms showing the mutations in cases 1–4. Shown are the direct sequences and subcloned normal and mutant sequences. The deleted sequences are shaded in *gray*, and the inserted sequence is highlighted in *yellow*. The mutant and the corresponding wild-type nucleotides are indicated by *red asterisks*.

detected by avidin conjugated to fluorescein isothiocyanate. To indicate an extent of a microdeletion, oligoarray comparative genomic hybridization (CGH) was carried out with 1×244K human genome array (catalog no. G4411B; Agilent Technologies, Palo Alto, CA), according to the manufacturer's protocol. Finally, to characterize a microdeletion, long PCR was performed with primer pairs flanking the deleted region, and a long PCR product was subjected to direct sequencing using serial sequence primers. The deletion size and the junction structure were determined by comparing the obtained sequences with the reference sequences at the National Center for Biotechnology Information Database (NC_000014.7; Bethesda, MD), and the presence or absence of repeat sequences around the breakpoints was examined with Repeatmasker (http://www.repeatmasker.org).

Functional studies

Western blot analysis, subcellular localization analysis, DNA binding analysis, and transactivation analysis were performed by the previously reported methods (8) (for details, see Supplemental Methods). In this study, we used the previously reported expression vector and fluorescent vector containing the wild-type *OTX2* cDNA; the probes with the wild-type and mutated OTX2 binding sites within the *IRBP*, *HESX1*, and *POU1F1* promoter sequences; and the luciferase reporter vectors containing the *IRBP*, *HESX1*, and *POU1F1* promoter sequences (8). We further created expression vectors and fluorescent vectors containing mutant *OTX2* cDNAs by site-directed mutagenesis using Prime STAR mutagenesis basal kit (Takara, Otsu, Japan), and constructed a 30-bp probe with wild-type (TAATCT) and mutated (TGGGCT) putative OTX2 binding site within the *GNRH1* promoter sequence and a luciferase reporter vector containing the *GNRH1* promoter sequence (−1349 to −1132 bp)

by inserting the corresponding sequence into pGL3 basic. The *GNRH1* promoter sequence was based on the report of Kelley *et al.* (15). Transfections were performed in triplicate within a single experiment, and the experiment was repeated three times.

PCR-based expression analysis of *OTX2*

Human cDNA samples were purchased from CLONTECH (Palo, Alto, CA) except for leukocyte and skin fibroblast cDNA samples that were prepared with Superscript III reverse transcriptase (Invitrogen). PCR amplification was performed for the cDNA samples (0.5 ng), using the primers hybridizing to exon 3 and 4 of *OTX2* and those hybridizing to exons 2/3 and 4/5 (boundaries) of *GAPDH* used as an internal control.

Results

Identification of mutations and substitutions

Three novel heterozygous *OTX2* mutations were identified in four cases, *i.e.* a 16-bp deletion at exon 4 that is predicted to cause a frameshift at the 74th codon for lysine and resultant termination at the 103rd codon (c.221_236del16, p.K74fsX103) in case 1; a 4-bp deletion and a 2-bp insertion at exon 4 that is predicted to cause a frame shift at the 72nd codon for alanine and resultant termination at the 86th codon (c.214_217delGCACinsCA, p.A72fsX86) in case 2; and a nonsense mutation at exon 5 that is predicted to cause a substitution of the 188th glycine with stop codon (c.562G>T, p.G188X) in two unrelated cases (3 and 4; Fig. 1). In addition, heterozygous missense substitutions were identified in patient 1 (c.532A>T, p.T178S) and patient 2 (c.734C>T, p.A245V). Cases 1 and 3 were from group 1, cases 2 and 4 and patient 2 were from group 2, and patient 1 was from group 3. Parental analysis indicated that frameshift mutations in cases 1 and 2 were absent from the parents (*de novo* mutations), whereas the missense substitution of patient 2 was inherited from phenotypically normal father. The parents of cases 3 and 4 and patient 1 refused molecular studies. All the mutations and the missense substitutions were absent from 100 control subjects.

Prediction of the occurrence of aberrant splicing and NMD

The two frameshift mutations and the nonsense mutation were predicted to influence neither exonic splice enhancers nor splice donor and acceptor sites (Supplemental Tables 2 and 3). Furthermore, the two frameshift mutations were predicted to produce the premature termination codons on the mRNA transcribed from the last exon
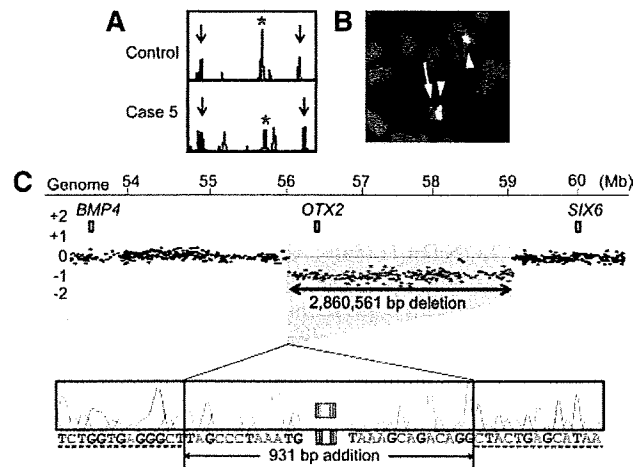
FIG. 2. Deletion analysis in case 5. A, MLPA analysis. The *red asterisk* indicates peaks for the *OTX2* exon 4, and the *black arrows* indicate control peaks. The *red peaks* indicate the internal size markers. Deletion of the MLPA probe binding site is indicated by the reduced peak height. B, FISH analysis. The probe for *OTX2* detects only a *single red signal* (an *arrow*), whereas the RP11-566I2 BAC probe identifies *two green signals* (*arrowheads*). C, Oligoarray CGH analysis and direct sequencing of the deletion junction. The deletion is 2,860,561 bp in physical size (shaded in *gray*) and is associated with an addition of a 931-bp segment (highlighted in *yellow*). The normal sequences flanking the microdeletion are indicated with *dashed underlines*.

5, indicating that the frameshift mutations as well as the nonsense mutation had the property to escape NMD (Supplemental Fig. 1).

Identification of a microdeletion

A heterozygous microdeletion affecting *OTX2* was indicated by MLPA and confirmed by FISH in case 5 of group 1 (Fig. 2, A and B). Oligoarray CGH delineated an approximately 2.9-Mb deletion, and sequencing of the fusion point showed that the microdeletion was 2,860,561 bp in physical size (56,006,531–58,867,091 bp on the NC_000014.7) and was associated with an addition of a complex 931-bp segment consisting of the following structures (cen → tel): 2 bp (TA) insertion → 895 bp sequence identical with that in a region just centromeric to the microdeletion (55, 911, 347–55, 912, 241 bp) → 1 bp (C) insertion → 33-bp sequence identical with that within the deleted region (58, 749, 744–58, 749, 776 bp) (Fig. 2C). Repeat sequences were absent around the break points. This microdeletion was not detected in DNA from the parents.

Functional studies of the wild-type and mutant OTX2 proteins

Western blot analysis detected wild-type OTX2 protein of 31.6 kDa and mutant OTX2 proteins of 11.5 kDa (p.K74fsX103), 9.7 kDa (p.A72fsX86), and 15.4 kDa (p.G188X) (Fig. 3A). The molecular masses were as predicted from the mutations. The band intensity was
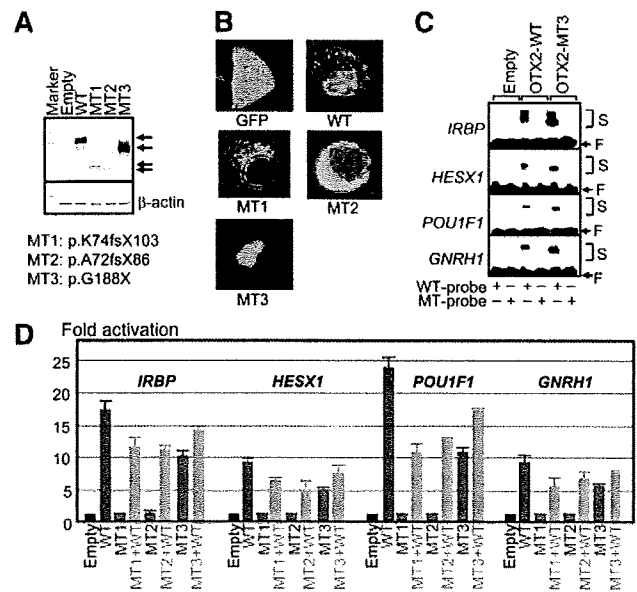

FIG. 3. Functional studies. A, Western blot analysis. Both WT and MT1-MT3 OTX2 proteins are detected with different molecular masses (*arrows*). WT, Wild type; MT1, p.K74fsX103; MT2, p.A72fsX86; and MT3, p.G188X. B, Subcellular localization analysis. Whereas green fluorescent protein (GFP) alone is diffusely distributed throughout the cell, the GFP-fused WT-OTX2 and MT3-OTX2 proteins localize to the nucleus. By contrast, the GFP-fused MT1-OTX2 and MT2-OTX2 proteins are incapable of localizing to the nucleus. C, DNA binding analysis using the wild-type (WT) and mutated (MT) probes derived from the promoters of *IRBP*, *HESX1*, *POU1F1*, and *GNRH1*. The symbols (+) and (−) indicate the presence and absence of the corresponding probes, respectively. Both WT and MT3 OTX2 proteins bind to the WT but not the MT probes. For the probe derived from the *IRBP* promoter, two shifted bands are found for both WT-OTX2 and MT3-OTX2 proteins as reported previously (17). S, Shifted bands; F, free probes. D, Transactivation analysis, using the promoter sequences of *IPBP*, *HESX1*, *POU1F1*, and *GNRH1*. The results are expressed using the mean and sd. The *black*, *blue*, *red*, and *green bars* indicate the data of the empty expression vectors (0.6 μg), expression vectors with WT *OTX2* cDNA (0.6 μg), expression vectors with MT1-MT3 *OTX2* cDNAs (0.6 μg), and the mixture of expression vectors with WT (0.3 μg) and those with MT1-MT3 *OTX2* cDNAs (0.3 μg), respectively; thus, the same amount of expression vectors has been used for each assay.

comparable between the wild-type OTX2 protein and the p.G188X-OTX2 protein and was faint for the p.K74fsX103-OTX2 and p.A72fsX86-OTX2 proteins.

Subcellular localization analysis showed that the p.G188X-OTX2 protein localized to the nucleus as did the wild-type OTX2 protein, whereas the p.K74fsX103-OTX2 and p.A72fsX86-OTX2 proteins were incapable of localizing to the nucleus (Fig. 3B). The results were consistent with those of the Western blot analysis because nuclear extracts were used for the Western blotting, with some probable contamination of cytoplasm.

DNA binding analysis revealed that the p.G188X-OTX2 protein with nuclear localizing capacity bound to the wild-type OTX2 binding sites within the four promoters examined, including the *GNRH1* promoter, but not to the mutated OTX2 binding sites (Fig. 3C). The band shift

−28−

A

B
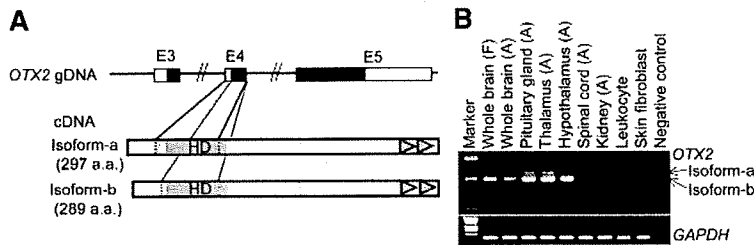
FIG. 4. PCR-based human cDNA library screening for OTX2 (35 cycles).
A, Schematic representation of the OTX2 isoform-a (NM_21728.2) and isoform-b
(NM_172337.1). Because of the two alternative splice acceptor sites at the boundary
between intron 3 and exon 4, isoform-a carries eight amino acids (shown in gray) in
the vicinity of the HD, whereas isoform-b is lacking the eight amino acids. B, PCR
amplification data. OTX2 is clearly expressed in the pituitary and hypothalamus, with
isoform-b being the major product. GAPDH has been used as an internal control.
F, Fetus; A, adult.

was more obvious for the wild-type OTX2 protein than for the p.G188X-OTX2 protein, consistent with the difference in the molecular masses.

Transactivation analysis showed that the wild-type OTX2 protein had transactivation activities for the four promoters examined including the GNRH1 promoter, whereas the p.K74fsX103-OTX2 and p.A72fsX86-OTX2 proteins had virtually no transactivation function, and the p.G188X-OTX2 protein had reduced (~50%) transactivation activities (Fig. 3D). The three mutant OTX2 proteins had no dominant-negative effects. In addition, the two missense p.A245V-OTX2 and p.T178S-OTX2 proteins had apparently normal transactivation activities with no dominant-negative effect (Supplemental Fig. 2).

PCR-based expression analysis of OTX2

OTX2 expression was identified in the pituitary and the hypothalamus as well as in the brain and the thalamus but not detected in the spinal cord, kidney, leukocytes, and skin fibroblasts (Fig. 4). The isoform-b lacking the eight amino acids was predominantly expressed.

Clinical findings in OTX2 mutation-positive patients

Clinical data are summarized in Table 1 (left part). Anophthalmia and/or microphthalmia was present in cases 1–5. Developmental delay was obvious in cases 1 and 3–5, whereas it was obscure in case 2 because of the young age. Prenatal growth was normally preserved in cases 1–5, whereas postnatal growth was compromised in cases 1, 3, and 5. Cases 1 and 5 had IGHD, and case 3 had CPHD (Table 2); furthermore, cases 1, 3, and 5 had pituitary hypoplasia (PH) and/or ectopic posterior pituitary (EPP) (Supplemental Fig. 3). Case 3 showed no pubertal development at 15 yr of age (Tanner pubic hair stage 2 in Japanese boys: 12.5 ± 0.9 yr) (16). Cases 2 and 4 had no discernible pituitary dysfunction and did not receive

magnetic resonance imaging examinations. In addition, case 1 had right retractile testis. Patient 1 with p.T178S had CPHD but without ocular anomalies, and patient 2 with p.A245V had bilateral optic nerve hypoplasia and short stature.

Discussion

We identified two frameshift mutations in cases 1 and 2 and a nonsense mutation in unrelated cases 3 and 4. Furthermore, it was predicted that these mutations neither affected splice patterns nor underwent NMD, although direct analysis using mRNA was impossible due to lack of detectable OTX2 expression in already collected leukocytes as well as skin fibroblasts, which might be available from cases 1–4. Thus, these mutations are predicted to produce aberrant OTX2 proteins in vivo that were used in the in vitro functional studies. In this context, the functional studies indicated that the two frameshift mutations were amorphic and the nonsense mutation was hypomorphic. The results are consistent with the previous notion that the HD not only has DNA binding capacity but also retains at least a part of nuclear localization signal on its C-terminal portion and the TD primarily resides in the C-terminal region (17) (Fig. 1A). Whereas the two missense substitutions were absent in 100 control subjects, they would be rare normal variations rather than pathological mutations because of the normal transactivation activities with no dominant-negative effect.

We also detected a heterozygous microdeletion involving OTX2 in case 5 that was not mediated by repeat sequences. This implies the importance of the examination of a microdeletion. Indeed, such a cryptic microdeletion has been identified in multiple genes with the development of MLPA that can serve as a screening method in the detection of microdeletions (18). Whereas the microdeletion of case 5 has removed 16 additional genes (Ensembl Genome Browser, http://www.ensembl.org/), the clinical phenotype of case 5 is explainable by OTX2 haploinsufficiency alone. Thus, hemizygosity for the 16 genes would not have a major clinical effect, if any.

Furthermore, the present study revealed two findings. First, OTX2 was expressed in the hypothalamus and had a transactivation function for the GNRH1 promoter. This implies that GNRH1 essential for the hypothalamic GnRH secretion is also a target gene of OTX2, as has been demonstrated in the mouse (15). Second, the short isoform-b was predominantly identified in the OTX2 expression-positive tissues. This sug-

TABLE 1. Summary of clinical findings in patients with heterozygous OTX2 mutations

	Present study						Previous studies[a]		
	Case 1	Case 2	Case 3	Case 4	Case 5	Case 6	Case 7	Case 8	Case 9
Present age (yr)	3	1	15	10	2	3	6	14	6
Sex	Male	Female	Male	Male	Male	Female	Male	Female	Male
Mutation[b] cDNA	c.221_236del	c.214_217del GCACinsCA	c.562G>T	c.562G>T	Whole gene deletion	c.402_403insC	c.674A>G	c.674A>G	c.405_406insCT
Protein	p.K74fsX103	p.A72fsX86	p.G188X	p.G188X	Absent	p.S135fsX136	p.N225S	p.N225S	p.S136fsX178
Function	Severe LOF	Severe LOF	Mild LOF	Mild LOF	Absent	Severe LOF	DN	DN	Severe LOF
Ocular malformation Right	AO	MO	MO	MO	MO	AO	N.D.	N.D.	AO
Left	MO	MO	MO	MO	AO	AO	N.D.	N.D.	AO
Developmental delay	+	Uncertain	+	+	+	+	N.D.	N.D.	+
Prenatal growth failure[c]	−	−	−	−	−	−	N.D.	N.D.	−
Birth length (cm) (SDS)	46.5 (−1.2)	48.3 (±0)	50 (+0.5)	49 (±0)	47.9 (−0.5)	50 (+0.6)	N.D.	N.D.	49.5 (+0.2)
Birth weight (kg) (SDS)	2.77 (−0.5)	3.22 (+0.6)	3.62 (+1.5)	3.23 (+0.5)	2.96 (−0.1)	3.16 (+0.2)	N.D.	N.D.	3.49 (+1.2)
Birth OFC (cm) (SDS)	32.5 (−0.7)	34 (+0.7)	N.E.	32.5 (−0.7)	31.5 (−1.4)	33.7 (+0.6)	N.D.	N.D.	N.D.
Postnatal growth failure[c]	+	−	+	−	+	+	+	+	+
Present height (cm) (SDS)	76.9 (−3.3)[d]	73.2 (±0)	114.0 (−4.1)[e]	130.8 (−1.5)	78.1 (−2.4)	85.0 (−3.3)	N.D.	N.D.	81.8 (−5.3)[f]
Present weight (kg) (SDS)	8.9 (−2.6)[d]	8.3 (−0.4)	16.8 (−2.4)[e]	23.2 (−1.6)	9.9 (−1.4)	10.1 (−2.6)	N.D.	N.D.	10.7 (−2.5)[f]
Present OFC (cm) (SDS)	N.E.	N.E.	N.E.	N.E.	N.E.	46 (−1.9)	N.D.	N.D.	47.2 (−2.7)[f]
Paternal height (cm) (SDS)[c]	160 (−1.9)	168 (−0.5)	178 (+1.2)	167 (−0.7)	163 (−1.3)	170 (±0)	178 (+0.3)	188 (+1.8)	N.D.
Maternal height (cm) (SDS)[c]	150 (−1.6)	151 (−1.3)	166 (+1.5)	165 (+1.4)	170 (+2.2)	155 (−0.6)	158 (−0.8)	168 (+0.7)	N.D.
Affected pituitary hormones	GH	No	GH, TSH, PRL, LH, FSH	No	GH	GH	GH, TSH, ACTH, LH, FSH	GH, TSH, ACTH, LH, FSH	GH, TSH, ACTH, LH, FSH
MRI findings Pituitary hypoplasia	+	N.E.	+	N.E.	+	−	+	+	+
EPP	+	N.E.	+	N.E.	−	−	+	−	+
Other features	Retractile testis (R)			Seizure		Cleft palate			Chiari malformation

SDS, sD score; OFC, occipitofrontal head circumference; MRI, magnetic resonance imaging; LOF, loss of function; DN, dominant negative; AO, anophthalmia; MO, microphthalmia; N.D., not described; N.E., not examined; PRL, prolactin; R, right.

[a] Case 6, Dateki et al. (8); cases 7 and 8, Diaczok et al. (9); case 9, Tajima et al. (10); [b] the cDNA and protein numbes are based on the human OTX2 isoform-b (GenBank accession no. NM_172337.1), and the A of the ATG encoding the initiator methionine residue is denoted position +1; thus, the description of the mutations in cases 7–9 is different from that reported by Diaczok et al. (9) and Tajima et al. (10); [c] assessed by the age- and sex-matched Japanese growth standards (27) (cases 1–6 and 9 and their parents) or by the American growth standards (28) (the parents of cases 7 and 8); [d] at 2 yr 4 months of age before GH treatment; [e] at 10 yr of age before GH treatment; [f] at 4 yr of age before GH treatment.

−30−

TABLE 2. Blood hormone values in cases 1–5 with heterozygous *OTX2* mutations

Patient Sex (age at examination)		Case 1 Male (2 yr)		Case 2 Female (1 yr)		Case 3 Male (14 yr)		Case 4 Male (10 yr)		Case 5 Male (2 yr)	
	Stimulus (dose)	Basal	Peak	Basal	Peak	Basal	Peak	Basal	Peak	Basal	Peak
GH (ng/ml)	Insulin (0.1 U/kg)[a]	1.9[b]	**4.0[b]**	3.3[b]	N.E.	0.8[b]	**1.3[b]**	12.1[b]	N.E.	0.5[c]	**9.0[c]**
	Arginine (0.5 g/kg)									1.1[c]	**7.0[c]**
	L-dopa (10 mg/kg)	1.5[b]	**3.8[b]**			0.3[b]	**1.0[b]**				
LH (mIU/ml)	GnRH (100 µg/m²)	0.1	1.7	0.1	N.E.	2.3[d]	4.5	0.4	N.E.	0.1	3.1
FSH (mIU/ml)	GnRH (100 µg/m²)	1.0	6.2	3.7	N.E.	1.3[d]	6.3	1.1	N.E.	1.5	9.9
TSH (µU/ml)	TRH (10 µg/kg)	4.2	23.8	1.1	N.E.	0.2	**1.9**	1.1	N.E.	5.2	19.5
Prolactin (ng/ml)	TRH (10 µg/kg)	17.9	34.5	N.E.	N.E.	5.5	**8.3**	9.1	N.E.	10.43	88.8
ACTH (pg/ml)	Insulin (0.1 U/kg)	31	195	N.E.	N.E.	24		N.E.	N.E.	41	222
Cortisol (µg/dl)[d]	Insulin (0.1 U/kg)	12.7		9.4	N.E.	19.4		N.E.	N.E.	25.4	39.2
IGF-I (ng/ml)		**8**		65	N.E.	**5**		214	N.E.	48	
Testosterone (ng/dl)		N.E.		N.E.	N.E.	**45**		<5	N.E.	N.E.	
Free T₄ (ng/dl)		1.32		1.17	N.E.	**0.87**		1.15	N.E.	1.17	
Free T₃ (pg/ml)		2.91		3.24	N.E.	**1.94**		3.92	N.E.	4.54	

The conversion factor to the SI unit: GH, 1.0 (µg/liter); LH, 1.0 (IU/liter); FSH, 1.0 (IU/liter); TSH, 1.0 (mIU/liter); prolactin, 1.0 (µg /liter); ACTH, 0.22 (pmol/liter); cortisol, 27.59 (nmol/liter); IGF-I, 0.131 (nmol/liter); testosterone, 0.035 (nmol/liter); free T_4, 12.87 (pmol/liter); and free T_3, 1.54 (pmol/liter). Hormone values have been evaluated by the age- and sex-matched Japanese reference data (29, 30); low hormone data are *boldfaced*. Blood sampling during the provocation tests: 0, 30, 60, 90, and 120 min. N.E., Not examined.

[a] Sufficient hypoglycemic stimulations were obtained during all the insulin provocation tests; [b] GH was measured using the recombinant GH standard, and the peak GH values of 6 and 3 ng/ml are used as the cutoff values for partial and severe GH deficiency, respectively; [c] GH was measured by the classic RIA, and the peak GH values of 10 and 5 ng/ml were used as the cutoff values for partial and severe GH deficiency; [d] Obtained at 0800–0900 h.

gests that the biological functions of *OTX2* are primarily contributed by the short isoform-b.

Clinical features of cases 1–5 are summarized in Table 1, together with those of the previously reported *OTX2* mutation-positive patients examined for detailed pituitary function. Here four patients with cytogenetically recognizable deletions involving *OTX2* are not included (19–22) because the deletions appear to have removed a large number of genes including *BMP4* and/or *SIX6* (Fig. 2B) that can be relevant to pituitary development and/or function (1, 23).

Several points are noteworthy for the clinical findings. First, although cases 1–5 in this study had anophthalmia and/or microphthalmia, ocular phenotype has not been described in cases 7 and 8 identified by *OTX2* mutation analysis in 50 patients with hypopituitarism (9). Whereas no description of a phenotype would not necessarily indicate the lack of the phenotype, *OTX2* mutations may specifically affect pituitary function at least in several patients. This would not be unexpected because several *OTX2* mutation-positive patients are free from ocular anomalies (6).

Second, pituitary phenotype is variable and independent of the *in vitro* function data. This would be explained by the notion that haploinsufficiency of developmental genes is usually associated with a wide range of penetrance and expressivity depending on other genetic and environmental factors (24), although the actual underlying factors remain to be identified. In this regard, because direct mRNA analysis was not performed, it might be possible

that the mutations have not produced the predicted aberrant protein and, consequently, *in vitro* function data do not necessarily reflect the *in vivo* functions. Even if this is the case, the quite different pituitary phenotype between cases 3 and 4 with the same mutation would argue for the notion that pituitary phenotype is independent of the residual OTX2 function.

Third, cases 1, 3, 5, and 6–9 with pituitary dysfunction have IGHD or CPHD involving GH, and show the combination of preserved prenatal growth and compromised postnatal growth characteristic of GH deficiency (25). This suggests that GH is the most vulnerable pituitary hormone in *OTX2* mutations. Consistent with this, previously reported patients with ocular anomalies and *OTX2* mutations also frequently exhibit short stature (6, 8). Thus, pituitary function studies are recommended in patients with ocular anomalies and postnatal short stature to allow for appropriate hormone therapies including GH treatment for short stature, cortisol supplementation at a stress period, T_4 supplementation to protect the developmental deterioration, and sex steroid supplementation to induce secondary sexual characteristics. Furthermore, *OTX2* mutation analysis is also recommended in such patients.

Lastly, PH and/or EPP is present in patients with IGHD and CPHD, except for case 6 with IGHD. In this regard, the following findings are noteworthy: 1) heterozygous loss-of-function mutations of *HESX1* are associated with a wide phenotypic spectrum including CPHD, IGHD, and apparently normal phenotype and often cause PH and

EPP, whereas homozygous *HESX1* mutations usually lead to CPHD as well as PH and EPP (2); 2) heterozygous loss-of-function mutations of *POU1F1* usually permit apparently normal pituitary phenotype, whereas homozygous loss-of-function mutations and heterozygous dominant-negative mutations usually result in GH, TSH, and prolactin deficiencies and often cause PH but not EPP (2); and 3) heterozygous *GNRH1* frameshift mutation are free from discernible phenotype, whereas homozygous *GNRH1* mutations result in isolated hypogonadotropic hypogonadism with no abnormal pituitary structure (26). Collectively, overall pituitary phenotype may primarily be ascribed to reduced *HESX1* expression, although reduced *POU1F1* and *GNRH1* expressions would also play a certain role, and there may be other target genes of *OTX2*.

In summary, the results imply that *OTX2* mutations are associated with variable pituitary phenotype, with no genotype-phenotype correlations, and that *OTX2* can transactivate *GNRH1* as well as *HESX1* and *POU1F1*. Further studies will serve to clarify the role of *OTX2* in the pituitary development and function.

Acknowledgments

References

1. Cohen LE, Radovick S 2002 Molecular basis of combined pituitary hormone deficiencies. Endocr Rev 23:431–442
2. Kelberman D, Dattani MT 2007 Hypopituitarism oddities: congenital causes. Horm Res 68(Suppl 5):138–144
3. Vieira TC, Boldarine VT, Abucham J 2007 Molecular analysis of PROP1, PIT1, HESX1, LHX3, and LHX4 shows high frequency of PROP1 mutations in patients with familial forms of combined pituitary hormone deficiency. Arq Bras Endocrinol Metab 51:1097–1103
4. Hever AM, Williamson KA, van Heyningen V 2006 Developmental

malformations of the eye: the role of *PAX6*, *SOX2* and *OTX2*. Clin Genet 69:459–470
5. Courtois V, Chatelain G, Han ZY, Le Novère N, Brun G, Lamonerie T 2003 New Otx2 mRNA isoforms expressed in the mouse brain. J Neurochem 84:840–853
6. Ragge NK, Brown AG, Poloschek CM, Lorenz B, Henderson RA, Clarke MP, Russell-Eggitt I, Fielder A, Gerrelli D, Martinez-Barbera JP, Ruddle P, Hurst J, Collin JR, Salt A, Cooper ST, Thompson PJ, Sisodiya SM, Williamson KA, Fitzpatrick DR, van Heyningen V, Hanson IM 2005 Heterozygous mutations of *OTX2* cause severe ocular malformations. Am J Hum Genet 76:1008–1022
7. Wyatt A, Bakrania P, Bunyan DJ, Osborne RJ, Crolla JA, Salt A, Ayuso C, Newbury-Ecob R, Abou-Rayyah Y, Collin JR, Robinson D, Ragge N 2008 Novel heterozygous OTX2 mutations and whole gene deletions in anophthalmia, microphthalmia and coloboma. Hum Mutat 29:E278–E283
8. Dateki S, Fukami M, Sato N, Muroya K, Adachi M, Ogata T 2008 OTX2 mutation in a patient with anophthalmia, short stature, and partial growth hormone deficiency: functional studies using the IRBP, HESX1, and POU1F1 promoters. J Clin Endocrinol Metab 93:3697–3702
9. Diaczok D, Romero C, Zunich J, Marshall I, Radovick S 2008 A novel dominant-negative mutation of OTX2 associated with combined pituitary hormone deficiency. J Clin Endocrinol Metab 93:4351–4359
10. Tajima T, Ohtake A, Hoshino M, Amemiya S, Sasaki N, Ishizu K, Fujieda K 2009 OTX2 loss of function mutation causes anophthalmia and combined pituitary hormone deficiency with a small anterior and ectopic posterior pituitary. J Clin Endocrinol Metab 94:314–319
11. Cartegni L, Chew SL, Krainer AR 2002 Listening to silence and understanding nonsense: exonic mutations that affect splicing. Nat Rev Genet 3:285–298
12. Strachan T, Read AP 2004 Instability of the human genome: mutation and DNA repair. In: Human molecular genetics. 3rd ed. London and New York: Garland Science; 334–337
13. Holbrook JA, Neu-Yilik G, Hentze MW, Kulozik AE 2004 Nonsense-mediated decay approaches the clinic. Nat Genet 36:801–808
14. Schouten JP, McElgunn CJ, Waaijer R, Zwijnenburg D, Diepvens F, Pals G 2002 Relative quantification of 40 nucleic acid sequences by multiplex ligation-dependent probe amplification. Nucleic Acids Res 30:e57
15. Kelley CG, Lavorgna G, Clark ME, Boncinelli E, Mellon PL 2000 The Otx2 homeoprotein regulates expression from the gonadotropin-releasing hormone proximal promoter. Mol Endocrinol 14:1246–1256
16. Matsuo N 1993 Skeletal and sexual maturation in Japanese children. Clin Pediatr Endocrinol 2(Suppl):1–4
17. Chatelain G, Fossat N, Brun G, Lamonerie T 2006 Molecular dissection reveals decreased activity and not dominant-negative effect in human OTX2 mutants. J Mol Med 84:604–615
18. den Dunnen JT, White SJ 2006 MLPA and MAPH: sensitive detection of deletions and duplications. Curr Protoc Hum Genet Chapter 7, Unit 7.14
19. Bennett CP, Betts DR, Seller MJ 1991 Deletion 14q (q22q23) associated with anophthalmia, absent pituitary, and other abnormalities. J Med Genet 28:280–281
20. Elliott J, Maltby EL, Reynolds B 1993 A case of deletion 14(q22.1→q22.3) associated with anophthalmia and pituitary abnormalities. J Med Genet 30:251–252
21. Lemyre E, Lemieux N, Décarie JC, Lambert M 1998 Del(14)(q22.1q23.2) in a patient with anophthalmia and pituitary hypoplasia. Am J Med Genet 77:162–165
22. Nolen LD, Amor D, Haywood A, St Heaps L, Willcock C, Mihelec M, Tam P, Billson F, Grigg J, Peters G, Jamieson RV 2006 Deletion at 14q22–23 indicates a contiguous gene syndrome comprising anophthalmia, pituitary hypoplasia, and ear anomalies. Am J Med Genet A 140:1711–1718

−32−

23. Zhu X, Lin CR, Prefontaine GG, Tollkuhn J, Rosenfeld MG 2005 Genetic control of pituitary development and hypopituitarism. Curr Opin Genet Dev 15:332–340
24. Fisher E, Scambler P 1994 Human haploinsufficiency — one for sorrow, two for joy. Nat Genet 7:5–7
25. Parks JS, Felner EI 2007 Hypopituitarism. In: Kliegman RM, Behrman RE, Jenson HB, Stanton BF, eds. Nelson textbook of pediatrics. 18th ed. Philadelphia: Saunders Elsevier; 2293–2299
26. Bouligand J, Ghervan C, Tello JA, Brailly-Tabard S, Salenave S, Chanson P, Lombès M, Millar RP, Guiochon-Mantel A, Young J 2009 Isolated familial hypogonadotropic hypogonadism and a GNRH1 mutation. N Engl J Med 360:2742–2748

27. Suwa S, Tachibana K, Maesaka H, Tanaka T, Yokoya S 1992 Longitudinal standards for height and height velocity for Japanese children from birth to maturity. Clin Pediatr Endocrinol 1:5–13
28. Kuczmarski RJ, Ogden CL, Guo SS, Grummer-Strawn LM, Flegal KM, Mei Z, Wei R, Curtin LR, Roche AF, Johnson CL 2002 2000 CDC growth charts for the United States: methods and development. Vital Health Stat 11 246:1–190
29. Japan Public Health Association 1996 Normal biochemical values in Japanese children (in Japanese). Tokyo: Sanko Press
30. Inada H, Imamura T, Nakajima R 2002 Manual of endocrine examination for children (in Japanese). Osaka: Medical Review

ORIGINAL ARTICLE

Problems in diagnosing atypical Gitelman's syndrome presenting with normomagnesaemia

Akinobu Nakamura*, Chikara Shimizu*, So Nagai*, Masahiro Yoshida*, Kazutaka Aoki†, Takuma Kondo*, Hideaki Miyoshi*, Norio Wada*, Toshihiro Tajima‡, Yasuo Terauchi†, Narihito Yoshioka* and Takao Koike*

*Department of Medicine II, Hokkaido University Graduate School of Medicine, Sapporo, Japan, †Department of Endocrinology and Metabolism, Graduate School of Medicine, Yokohama City University, Yokohama, Japan and ‡Department of Pediatrics, Hokkaido University Graduate School of Medicine, Sapporo, Japan

Summary

Objective Gitelman's syndrome, recognized as a variant of Bartter's syndrome, is characterized by hypokalaemic metabolic alkalosis in combination with hypomagnesaemia and hypocalciuria. Overlapping biochemical features in Gitelman's syndrome and Bartter's syndrome has been observed. Here, we investigated the clinical, biochemical, and genetic characteristics of five, chronic, nonhypertensive and hypokalaemic Japanese patients.

Methods Serum and urinary electrolytes, plasma renin activity and plasma aldosterone concentration were measured in five patients (four males and one female) with hypokalaemia. Renal clearance tests were performed and distal fractional chloride reabsorption calculated. Finally, mutational analysis of the thiazide-sensitive Na-Cl co-transporter gene was performed.

Results Symptoms in patients varied from mild (muscle weakness and numbness) to severe (tetany and foot paralysis). All patients were normotensive or hypotensive, and all had hypokalaemia, hypocalciuria, and hyperreninaemic hyperaldosteronism. However, two male patients had normomagnesaemia, while the remainder was hypomagnesaemic. Renal clearance tests showed that the administration of furosemide decreased distal fractional chloride reabsorption, while thiazide ingestion failed to decrease it. Genetic analysis identified six thiazide-sensitive Na-Cl co-transporter gene mutations, including two novel ones. Therefore, on the basis of the confirmatory renal clearance tests and mutational analysis, a diagnosis of Gitelman's syndrome was made in these patients.

Conclusions Two of the five patients diagnosed with Gitelman's syndrome were normomagnesaemic, which is uncommon in this syndrome. Our study indicates that renal clearance tests and mutation analysis can play an important role in diagnosing Gitelman's syndrome more precisely.

Correspondence: Chikara Shimizu, Department of Medicine II, Hokkaido University Graduate School of Medicine, N-15, W-7, Kita-ku, Sapporo 060-8638, Japan. Tel: +81-11-706-5915; Fax: +81-11-706-7710; E-mail: shimizch@med.hokudai.ac.jp

Introduction

Gitelman's syndrome (GS), recognized as a variant of Bartter's syndrome (BS), is characterized by hypokalaemic metabolic alkalosis in combination with hypomagnesaemia and hypocalciuria.[1] Patients with GS are usually diagnosed in adulthood during routine investigation, generally presenting with mild symptoms including cramps and fatigue, although some suffer from severe symptoms such as tetany, paralysis and rhabdomyolysis.[2] GS is frequently associated with inactivating mutations in the thiazide-sensitive Na-Cl cotransporter (*TSC*) gene,[3] also referred to as *SLC12A3*, and to date, more than 100 distinct *TSC* gene mutations have been identified in GS.[4] Frequently, assessments of urinary calcium excretion and serum levels of magnesium are used to biochemically differentiate between GS and BS.[5,6] Although patients with GS and BS in general have normal serum calcium levels, those with BS typically have normal or increased urinary calcium excretion, whereas GS is characterized by hypocalciuria.[5] Moreover, 60–70% of BS patients have normomagnesaemia, whereas most patients with GS have hypomagnesaemia.[5,6] However, overlapping of biochemical parameters between patients with GS and BS has been observed.[7,8]

In the present study, we investigated the clinical, biochemical, and genetic characteristics of five chronic nonhypertensive and hypokalaemic Japanese patients. Six *TSC* gene mutations, including two novel mutations, were identified. Two male patients with hypokalaemia and mutations in *TSC* were normomagnesaemic. Our results provide evidence of the importance of using renal clearance tests and mutation analysis to diagnose GS more precisely.

Methods

Patients

This study included five patients (four males and one female) with hypokalaemia from Hokkaido University Hospital, Sapporo Shakai

272

Hoken General Hospital, Sapporo City Hospital, Takikawa City Hospital in Hokkaido, and Yokohama City University Hospital in Yokohama, Japan. The details of two males and one female (patients 1, 2 and 3) were described previously.[9-11] All five patients were on normal diets and not taking either regular medications or supplements that could affect serum electrolytes. Serum and urinary electrolytes, plasma renin activity (PRA) and plasma aldosterone concentration (PAC) were measured by standard laboratory techniques. Four of the five patients underwent renal clearance tests as described below. Genetic analysis was made following the approval of the institutional review board and written informed consent by the patients.

Renal clearance tests

Renal clearance tests were performed according to a previously described protocol.[12] Briefly, the patients ingested water (20 ml/kg body weight) after an overnight fast then received an intravenous infusion of 0·45% saline. Once the urinary flow reached a rate of 10 ml/min, either furosemide (20 mg intravenously) or hydrochlorothiazide (100 mg orally) was administered. Clearance was calculated as follows: osmolar clearance (Cosm) = $Uosm \times V/Posm$, where V is the urine volume; the maximal free water clearance $(CH_2O) = V - Cosm$; chloride clearance (CCl) = $UCl \times V/PCl$; and distal fractional chloride reabsorption (DFCR) is defined as $CH_2O/(CH_2O + CCl)$.

Mutational analysis

Genomic DNA was isolated and purified from whole blood and oligonucleotide primers were used to generate PCR products from all 26 exons of the *TSC* gene as described in a previous report.[13] Amplified products were subjected to direct sequencing. AmpliTaq-Gold (PE Applied Biosystems, Foster City, CA, USA) and its standard buffer were used in all reactions. PCRs were carried out under the following conditions: initial denaturation at 95 °C for 7 min, followed by 30 cycles at 94 °C for 1 min, 65 °C for 1 min, and 72 °C for 1 min. PCR products were purified by low melting agarose gel electrophoresis and subjected to automated sequencing according to the manufacturer's protocol (PE Applied Biosystems, Model 373A DNA sequencer, Foster City, UA, USA).

Results

Clinical features

Four males and one female, ranging in age from 18 to 56 years, were included in the study (Table 1). The patients were asymptomatic throughout infancy with no history of renal stones or nephrocalcinosis. Their symptoms at presentation varied from mild (muscle weakness and numbness) to severe (tetany and foot paralysis). One male (patient 4) was asymptomatic and hypokalaemia was identified by a routine medical examination. All patients were normotensive (patients 1 and 5) or rather hypotensive (patients 2, 3 and 4) for their age and gender (Table 1).

Biochemical data

Patient biochemical data are summarized in Table 2. All had hypokalaemia (K^+ 1·7 to 3·5 mmol/l, reference range 3·6–5·4), and their renal function as assessed by serum creatinine was normal (data not shown). Urine calcium to creatinine ratios were depressed (u-Ca^{2+}/Cr 0·002 to 0·115), and PRA and PAC were elevated (PRA 1·1 to 5·6 ng/l·s, reference range 0·1–0·8; PAC 555 to 788 pmol/l, reference range 83–164). These data are consistent with a clinical diagnosis of GS.[5,14] However, two male patients (patients 4 and 5) were normomagnesaemic (Mg^{2+} 0·7 and 0·9 mmol/l, reference range 0·7–1·1), which is pathognomonic for BS rather than GS, whereas the others (patients 1, 2 and 3) were hypomagnesaemic (Mg^{2+} 0·2 to 0·5 mmol/l).

Clearance tests

Since the clinical features and electrolyte imbalances indicated by the biochemical studies were attributable to GS, a renal clearance test using furosemide or thiazide was carried out in four of the patients (patients 1, 3, 4 and 5). In one patient (patient 2), a renal clearance test could not be carried out because it was difficult to obtain her cooperation due to her mental retardation. The DFCR results are shown in Table 3. In all four patients, administration of furosemide decreased DFCR, while thiazide ingestion failed to decrease DFCR. These results indicate that the thick ascending limb of Henle's loop, which is targeted by furosemide, is functionally intact, and that the function of the thiazide-sensitive distal

Table 1. Clinical features of patients

| Patient | Gender | Age (years) | Blood pressure | | Manifestations |
			mmHg	Reference range	
1	Male	18	128/78	(113 ± 13/66 ± 9)	Muscle weakness, tetany
2	Female	56	110/70	(131 ± 19/80 ± 11)	Headache, foot paralysis
3	Male	52	118/72	(136 ± 19/85 ± 11)	Sleeplessness, tinnitus
4	Male	39	106/60	(123 ± 13/78 ± 11)	No symptom
5	Male	27	110/82	(120 ± 14/74 ± 11)	Muscle weakness, numbness

Reference ranges show age and gender-specific means ± SD.

Table 2. (a) Biochemical data of patients – circulating biochemical features. (b) Biochemical data of patients – urinary biochemical features

Patient	Na^+ (mmol/l)	K^+ (mmol/l)	Cl^- (mmol/l)	Mg^{2+} (mmol/l)	PRA (ng/l·s)	PAC (pmol/l)	pH	HCO_3^- (mmol/l)
(a)								
1	142	3·5	99	0·2	1·1	555	7·42	25·5
2	140	1·7	90	0·5	5·6	583	7·59	41·6
3	143	2·6	90	0·5	4·2	685	7·45	32·3
4	139	2·9	97	0·9	3·9	788	7·44	31·7
5	141	3·1	97	0·7	4·4	755	7·46	28·9
Reference range	136–147	3·6–5·4	98–109	0·7–1·1	0·1–0·8	83–164	7·35–7·45	23–28

Patient	$u\text{-}Na^+$ (mmol/day)	$u\text{-}K^+$ (mmol/day)	$u\text{-}Cl^-$ (mmol/day)	$u\text{-}Ca^{2+}$ (mmol/day)	$u\text{-}Ca^{2+}/Cr$ (mmol/mmol)
(b)					
1	81·0	43·1	73·5	0·04	0·002
2	98·8	22·4	123·5	0·45	0·115
3	167·6	77·1	174·3	1·45	0·110
4	67·5	62·7	94·3	1·26	0·000
5	135·0	63·2	165·0	0·87	0·003

PRA, plasma renin activity; PAC, plasma aldosterone concentration.
$u\text{-}Ca^{2+}/Cr$, molar ratio of urinary calcium to creatinine.

Table 3. Distal fractional chloride reabsorption tests

	Thiazide administration		Furosemide administration	
Patient	Pre (%)	Post (%)	Pre (%)	Post (%)
1	85·2	75·7	77·7	19·4
2	ND	ND	ND	ND
3	72·2	72·6	70·6	22·6
4	86·5	71·4	84·9	16·9
5	61·0	58·2	60·8	42·5

ND, not determined.

convoluted tubule is impaired. A clinical diagnosis of GS was made on the basis of clinical features, laboratory data and renal clearance tests in these four patients.

Mutational analysis of the TSC gene

To evaluate the potential of genetic tests to diagnose GS more precisely, mutational analysis of the TSC gene was carried out to supplement the clinical observations. All 26 exons of *TSC* were amplified from patient genomic DNA by PCR, then directly sequenced in their entirety. Six different mutations, including three novel mutations, were identified (Table 4). Patient 1 is heterozygous for a C to A nucleotide transversion at nucleotide position 545 in exon 4, causing a predicted Thr to Lys substitution at codon 180. No other mutations were identified on either allele were in this individual. Patient 2, who did not undergo a renal clearance test study, is homozygous for a T for C transition at nucleotide position 1930 in exon 15, resulting in a predicted Arg to Cys missense mutation at codon 642. On the basis of this previously reported

Table 4. Thiazide sensitive co-transporter (*TSC*) mutations

Patient	Location	Mutation
1	Exon 4	Thr180Lys (Heterozygosity)
2	Exon 15	Arg642Cys (Homozygosity)
3	Exon 1	c1A>T (Homozygosity)
4	Exon 22/25	Leu858His/Ser976Phe (Compound heterozygosity)
5	Exon 22/25	Leu858His/Arg964Gln (Compound heterozygosity)

mutation,[15] a diagnosis of GS was confirmed in patient 2. Patient 3 is homozygous for a T to A transversion in the initial codon of exon 1 (c1A>T), resulting in a predicted missense mutation. Patients 4 and 5 are both compound heterozygotes for three different mutations. A T to A transversion at nucleotide position 2579 in exon 22 is common to both patients, and causes a predicted Leu to His substitution at codon 858. Patient 4 is also heterozygous for a C to T transition at nucleotide position 2933 in exon 25, resulting in a predicted substitution of Ser for Phe at codon 976. Finally, patient 5 is also heterozygous for a G to A transition at nucleotide position 2897 in exon 25, which is predicted to substitute Arg for Glu at codon 964. None of the two mutations (Leu858His and Ser976Phe) identified in patients 4 and 5 have been previously described. Direct sequencing did not identify these mutations in any of 25 unrelated healthy subjects.

Discussion

Once vomiting, diuretic and laxative abuse are excluded from the differential diagnosis of a nonhypertensive patient presenting with hypokalaemia, rare conditions such as renal tubular acidosis, BS or

GS need to be considered. BS and GS have many clinical features in common, such as hypokalaemic alkalosis, salt wasting, and normotension or hypotension despite elevated levels of plasma renin and aldosterone.[16] The overlapping physiological features and phenotypic variability of these disorders has resulted in confusion regarding their classification. Clinically, the two have been distinguished based on serum magnesium and urinary calcium findings,[5,6] with GS denoting the subset characterized by hypomagnesaemia and hypocalciuria. An additional subset, namely patients with BS who present neonatally and typically have nephrocalcinosis, has been recognized.[17] Patients with BS typically present before the age of six with severe symptoms such as dehydration and growth retardation. In contrast, patients with GS typically present in early adulthood and with predominantly neuromuscular symptoms. Some of these patients experience severe fatigue that interferes with daily activities, whereas others never complain of tiredness.[18] According to Bettinelli *et al.*,[5,14] clinical criteria diagnostic of Gitelman's syndrome are hypomagnesaemia, hypokalaemia, and hypocalciuria. In our study, three cases (patients 1, 2, and 3) met these criteria, however two male patients (patient 4 and 5) were normomagnesaemic.

Normomagnesaemia has been reported in some patients with GS due to *TSC* mutations.[19-23] Although the causes of normomagnesaemia in patients with *TSC* mutations have remained elusive, a recent study by Lin *et al.*[24] has shed some light on the issue. They reported two families with molecularly proven GS, in which male patients had normal serum magnesium. Remarkably, female GS patients within these families, who carried the same TSC mutations as the male patients, had hypomagnesaemia. Although this study was small, the authors concluded that gender may affect clinical parameters in GS. In our study, the two normomagnesaemic patients were also male. These data substantiate the possibility that gender may play an important role in the regulation of both TSC and the transient-receptor potential channel subfamily M, member 6 (TRPM6). TRPM6 is a magnesium-permeable channel localized along the apical membrane of the distal convoluted tubule, to which active magnesium reabsorption is restricted.[25] Nijenhuis *et al.*[26] concluded that reduced TRPM6 expression and the resulting defect in active magnesium reabsorption in the distal convoluted tubule may represent a general mechanism in the pathogenesis of hypomagnesaemia that accompanies GS. In studies in rats, TSC expression in the distal convoluted tubule is subject to control by sex hormones, leading to alterations in renal excretion of electrocytes.[27] TRPM6 has also been shown to be regulated by oestrogens in rats.[28] Nevertheless, other factors regulating the function of the TSC and TRPM6 channels should be investigated as possible explanations for the clinical variability of GS.

In the four male patients in the current study, renal clearance tests showed that while the furosemide-sensitive segment of the thick ascending limb of the loop of Henle was functionally intact, the thiazide-sensitive segment of the distal convoluted tubule was not, indicating a specific defect in TSC function. Although some reports have shown that mutations in the kidney-specific basolateral chloride channel (*CLCNKB*) gene could cause a mixed diagnosis of GS and BS,[29,30] mutation of *TSC* was preferentially expected on the basis of renal clearance test. We confirmed GS by identification of TSC gene mutations in these patients.

To date, more than 100 different *TSC* gene mutations, including missense, nonsense, frameshift, deletion, insertion and splice site mutations have been identified in patients with GS.[4] These mutations are distributed throughout the coding sequence of *TSC*, but occur most frequently in the intracellular domains of the protein.[31] Missense mutations are the most common reported abnormality, and we identified six such mutations in our GS patients. Among these mutations, four of the six were localized in the intracellular cytoplasmic carboxyl terminus. The mutations identified in patients 1 and 2 are common mutations in Japanese GS patients.[15,32] Although *TSC* in patient 2 had a homozygous missense mutation (Arg642Lys), patient 1 had a heterozygous missense mutation (Thr180Lys). We speculate that patient 1 may have an unidentified gene abnormality on the allele in addition to the Thr180Lys mutation.[9] The functional consequence of the mutation in patient 3 is unknown, however it may be speculated that this mutation might change amino acid residues due to alternative initiation of translation at a second, in-frame ATG present 53 codons downstream, potentially impairing the function of the TSC protein.[11] Patients 4 and 5 were compound heterozygous for two different mutations on both TSC alleles, which is the most common inheritance pattern in GS patients.[22,23] Although Leu858His and Ser976Phe, which were identified in the two patients, have not been previously described, these are novel mutations but not single nucleotide polymorphisms (SNP's) considering the direct sequencing results of unrelated healthy subjects. Because renal TSC in these patients was deficient as indicated by the results of the renal clearance test, these mutations may affect TSC function, although functional studies would be required to state this definitively. Although these patients were uncommon in having normomagnesaemia, evidence suggests that this condition is associated not with these TSC mutations but with other factors such as gender, as described above.

In summary, we investigated the clinical, biochemical and genetic characteristics of five chronic nonhypertensive and hypokalaemic Japanese patients. Two out of five patients diagnosed as GS were normomagnesaemic, which is uncommon in GS. For more precise diagnosis of GS, we suggest that renal clearance tests and mutational analysis be carried out routinely.

Acknowledgement

Competing interests/financial disclosure

All have nothing to declare.

References

1 Gitelman, H., Graham, J. & Welt, L. (1966) A new familial disorder characterized by hypokalemia and hypomagnesemia. *Transactions of the Association of American Physicians*, 79, 92–96.

2 Cruz, D.N., Shaer, A.J., Bia, M.J. *et al.* (2001) Gitelman's syndrome revisited: an evaluation of symptoms and health-related quality of life. *Kidney International*, 59, 710–717.

3 Simon, D.B., Nelson, W.C., Bia, M.J. *et al.* (1996) Gitelman's variant of Bartter's syndrome, inherited hypokalemic alkalosis, is caused by mutations in the thiazide-sensitive Na-Cl cotransporter. *Nature Genetics*, 12, 24–30.

4 Gamba, G. (2005) Molecular physiology and pathophysiology of electroneutral cation-chloride cotransporters. *Physiological Reviews*, 85, 423–493.

5 Bettinelli, A., Bianchetti, M.G., Girardin, E. *et al.* (1992) Use of calcium excretion values to distinguish two forms of primary renal tubular hypokalemic alkalosis: Bartter and Gitelman syndromes. *Journal of Pediatrics*, 120, 38–43.

6 Stein, J.H. (1985) The pathogenetic spectrum of Bartter's syndrome. *Kidney International*, 28, 85–93.

7 Turman, M.A. (1998) Concomitant occurrence of Gitelman and Bartter syndromes in the same family? *Pediatric Nephrology*, 12, 23–25.

8 Simon, D.B. & Lifton, R.P. (1996) The molecular basis of inherited hypokalemic alkalosis: Bartter's and Gitelman's syndromes. *The American Journal of Physiology Society*, 271, F961–F966.

9 Nakamura, A., Shimizu, C., Nagai, S. *et al.* (2005) A rare case of Gitelman's syndrome presenting with hypocalcemia and osteopenia. *Journal of Endocrinological Investigation*, 28, 464–468.

10 Morita, R., Takeuchi, K., Nakamura, A. *et al.* (2006) Gitelman's syndrome with mental retardation. *Internal Medicine*, 45, 211–213.

11 Aoki, K., Tajima, T., Yabushita, Y. *et al.* (2008) A novel initial codon mutation of the thiazide-sensitive Na-Cl cotransporter gene in a Japanese patient with Gitelman's syndrome. *Endocrine Journal*, 55, 557–560.

12 Tsukamoto, T., Kobayashi, T., Kawamoto, K. *et al.* (1995) Possible discrimination of Gitelman's syndrome from Bartter's syndrome by renal clearance study: report of two cases. *American Journal of Kidney Diseases*, 25, 637–641.

13 Tajima, T., Kobayashi, Y., Abe, S. *et al.* (2002) Two novel mutations of thiazide-sensitive Na-Cl cotransporter (TSC) gene in two sporadic Japanese patients with Gitelman's syndrome. *Endocrine Journal*, 49, 91–96.

14 Bettinelli, A., Bianchetti, M.G., Borella, P. *et al.* (1995) Genetic heterogeneity in tubular hypomagnesemia-hypokalemia with hypocalciuria (Gitelman's syndrome). *Kidney International*, 47, 547–551.

15 Yahata, K., Tanaka, I., Kotani, M. *et al.* (1998) Identification of a novel R642C mutation in Na/Cl cotransporter with Gitelman's syndrome. *American Journal of Kidney Diseases*, 34, 845–853.

16 Naesens, M., Steels, P., Verberckmoes, R. *et al.* (2004) Bartter's and Gitelman's syndromes: from gene to clinic. *Nephron Physiology*, 96, 65–78.

17 Proesmans, W. (1997) Bartter syndrome and its neonatal variant. *European Journal of Pediatrics*, 156, 669–679.

18 Knoers, N.V. (2006) Gitelman syndrome. *Advances in Chronic Kidney Disease*, 13, 148–154.

19 Takeuchi, K., Kato, T., Taniyama, Y. *et al.* (1997) Three cases of Gitelman's syndrome possibly caused by different mutations in the thiazide-sensitive Na-Cl cotransporter. *Internal Medicine*, 36, 582–585.

20 Fukuyama, S., Okudaira, S., Yamazato, S. *et al.* (2003) Analysis of renal tubular electrolyte transporter genes in seven patients with hypokalemic metabolic alkalosis. *Kidney International*, 64, 808–816.

21 Yoo, T., Lee, S., Yoon, K. *et al.* (2003) Identification of novel mutations in Na-Cl cotransporter gene in a Korean patient with atypical Gitelman's syndrome. *American Journal of Kidney Diseases*, 42, 11–16.

22 Maki, N., Komatsuda, A., Wakui, H. *et al.* (2004) Four novel mutations in the thiazide-sensitive Na-Cl co-transporter gene in Japanese patients with Gitelman's syndrome. *Nephrology, Dialysis, Transplantation*, 19, 1761–1766.

23 Lin, S.H., Shiang, J.C., Huang, C.C. *et al.* (2005) Phenotype and genotype analysis in Chinese patients with Gitelman's syndrome. *Journal of Clinical Endocrinology and Metabolism*, 90, 2500–2507.

24 Lin, S.H., Chenq, N.L., Hsu, Y.J. *et al.* (2004) Intrafamilial phenotype variability in patients with Gitelman syndrome having the same mutations in their thiazide-sensitive sodium/chloride cotransporter. *American Journal of Kidney Diseases*, 43, 304–312.

25 Schlingmann, K.P. & Gudermann, T. (2005) A critical role of TRPM channel-kinase for human magnesium transport. *Journal of Physiology*, 566, 301–308.

26 Nijenhuis, T., Vallon, V., van der Kemp, A.W. *et al.* (2005) Enhanced passive Ca^{2+} reabsorption and reduced Mg^{2+} channel abundance explains thiazide-induced hypocalciuria and hypomagnesemia. *Journal of Clinical Investigation*, 115, 1651–1658.

27 Chen, Z., Vaughn, D.A. & Fanestil, D.D. (1994) Influence of gender on renal thiazide diuretic receptor density and response. *Journal of the American Society of Nephrology*, 5, 1112–1119.

28 Groenestege, W.M., Hoenderop, J.G., van den Heuvel, L. *et al.* (2006) The epithelial Mg2 + channel transient receptor potential melastatin 6 is regulated by dietary Mg2 + content and estrogens. *Journal of the American Society of Nephrology*, 17, 1035–1043.

29 Jeck, N., Konrad, M., Peters, M. *et al.* (2000) Mutations in the chloride channel gene, CLCNKB, leading to a mixed Bartter-Gitelman phenotype. *Pediatric Research*, 48, 754–758.

30 Zelikovic, I., Szargel, R., Hawash, A. *et al.* (2003) A novel mutation in the chloride channel gene, CLCNKB, as a cause of Gitelman and Bartter syndromes. *Kidney International*, 63, 24–32.

31 Reissinger, A., Ludwig, M., Utsch, B. *et al.* (2002) Novel NCCT gene mutations as a cause of Gitelman's syndrome and a systematic review of mutant and polymorphic NCCT alleles. *Kidney & Blood Pressure Research*, 25, 354–362.

32 Monkawa, T., Kurihara, I., Kobayashi, K. *et al.* (2000) Novel mutations in thiazide-sensitive Na-Cl cotransporter gene of patients with Gitelman's syndrome. *Journal of the American Society of Nephrology*, 11, 65–70.

食行動異常による成長障害

田島敏広*

はじめに

食行動の異常として摂食障害がある。この摂食障害（中枢性摂食異常症）は心理的要因で食行動の異常を示す疾患であり，そのなかでも神経性食欲不振症（anorexia nervosa：AN）が代表的疾患である。その成因はさまざまな因子がからみあっており，社会的要因，心理的傾向，遺伝的性格形質などが関与する。体重や体型について歪んだ認識が根底にあり，やせ願望，体重増加への恐怖から摂食を行わず，極端なるいそう状態になる。そのため慢性的なストレスに陥り，内分泌代謝異常を起こす。その成長については，過去の報告では栄養不良，内分泌代謝異常によって，低身長になると考えられていた[1]。今回，AN の内分泌代謝の異常や AN の成長障害について述べる。

1 内分泌代謝異常

厚生労働省特定疾患研究班の AN の診断基準は，1）標準体重の－20％のやせが 3 か月以上持続する，2）小食，多食，隠れ食いなどの食行動の異常，3）体重，体型についての歪んだ認識，4）発症年齢は 30 歳以下，5）女性ならば無月経があり，やせの原因と考えられる器質的疾患，精神疾患がないとされている[2]。

AN の内分泌異常を表にまとめた。視床下部－下垂体－副腎系については，活性の亢進がみられ

表　神経性食欲不振症の内分泌異常

成長ホルモン系
　GH 分泌亢進または GH 分泌不全
　IGF-1 の低値

性腺系
　LH 低値
　FSH 低値〜正常
　E2 の低値

副腎皮質系
　cortisol の分泌亢進
　日内変動の消失
　脳脊髄液の CRH の増加

甲状腺系
　T_3の低値
　リバース T_3の増加

脂質系
　レプチン低値

る[3,4]。食行動の異常，精神的，心理的ストレスによって，視床下部 CRH（コルチコトロピン放出ホルモン）が過剰産生され，その結果血中コルチゾール値は上昇している[3,4]。

視床下部－下垂体－性腺系については性腺刺激ホルモンの分泌障害があり，レプチンの低下により GnRH（ゴナドトロピン放出ホルモン）の分泌が低下している可能性もある。視床下部－下垂体甲状腺系も抑制されており，血中 T_4値は正常下限，T_3は低値，リバース T_3は上昇し，いわゆる low T_3症候群を呈している[4]。成長ホルモン（GH）系で GH 抵抗性が報告されている[5]。GH の基礎分泌，夜間の GH のパルス分泌は増加しているが，GH により産生が増加する血中 GH 結合蛋白，血中 IGFBP-3 は低下している。堀川らは 10〜1 歳の 36 名の日本人 AN で GH 分泌を検討しているが，約半数が夜間分泌増加，GH 負荷試験で

Tajima Toshihiro
* 北海道大学医学部小児科
〔〒060-8638　札幌市北区北 15 条西 7 丁目〕
TEL 011-716-1161　FAX 011-706-7898
E-mail：tajeari@med.hokudai.ac.jp

過剰分泌を示したが,約半数ではGHの分泌は低下していたと報告している[6]。低栄養状態であるため,血中IGF-1は低下していることがほとんどである。

現時点でこのような内分泌系の異常が存在しても,甲状腺ホルモン補充,性腺ホルモン補充は行わない。

5 成　長

ANの成長,身長については目標身長よりも低くなると考えられていたが[1,7,8],最近ではほぼ目標身長に到達するとの報告もある。しかし,成人身長まで経過観察し,正常コントロールと比較した報告は諸外国も含めてすくない。Lantozini らは12～17歳までの16名のAN女性の成人身長までのデータを報告している[9]。治療により体重が増加した場合,月経が再開し,身長のcatch-upが起こったが,その伸び率は正常女性に比較し,少なかったとしている。その結果16名中13名で,目標身長に比べ平均4.1±3.6cm低かった。またRozeらは33名の女性のANについて検討を行っている[10]。ANの診断の年齢は平均11.8歳で,その後21歳での身長を検討している。患者は治療により初経が平均15.4歳に出現していた。33名中21名は目標身長に到達したが,残りの12名は目標身長より平均3.9cmほど低かった。この研究ではANの発症年齢,月経の出現時期は成人身長と関連しなかったが,入院期間が長いほど身長は低い,つまり重症なほど身長が低くなる結果であった。

Prabkaharanらは AN女性110名(12～18歳)と対象の同年齢の女性98例の身長,成長について比較検討している[5]。ANの罹病期間は11.6±13.2か月である。その報告によれば,最初の診断時の身長,身長SDSは正常コントロールに比較し,有意に低下していなかった。この時点での予測成人身長も正常コントロールに比較し,有意な低下は認めなかった。ただし,罹病期間が長い症例ほど身長SDSが低く,予測成人身長は低かった。さらに,AN63名の1年間の成長について同年齢女性と比較している。その結果は,1年間の

身長の伸び率はANでは少ない傾向にあったが,正常コントロールに比較して,有意差を認めるほどではなかった。骨年齢が暦年齢に遅れているほど,1年間の身長のSDSの改善は良好であった。この骨年齢の遅れは性腺機能低下によるエストロゲン分泌不全によるものと考えられる。したがって,少なくとも短期間の身長の伸びについては骨年齢の遅れによって,代償できる可能性が示された。検討対象の症例数は多いが,この論文の著者らも述べているように,ANの診断治療に入るまでの期間が他の研究に比べて短いため,より軽症な症例のみに偏っている可能性があること,また観察期間が1年と短期間であり,成人身長まで追跡が行われていない点に留意する必要がある。

ANの男子における成長についての検討は少ない。Siegelらは10名のANで検討し,成人身長が低かったと報告している[11]。Modan-Moseseらは12人の男子のANについてその成長を報告している[12]。入院年齢は14.3±1.5歳で症状の発現期間は12.4±11.1か月であった。その後,38.4±19.4か月フォローしている。その結果,疾患発症前の身長SDSは-0.21±0.91であったが,入院時は-0.8±-0.93と有意に低下していた。引き続き成人身長までフォローできたのは8名であるが,入院治療により,体重増加,急速な身長の伸びを認めたが,成人身長のSDSは-0.52±0.84であり,目標身長よりも低い傾向にあった。

日本では堀田らが14歳未満で発症したAN患者の成人身長,成人身長に影響を与える因子について検討している[13]。18歳までに体重,月経が回復した22名の患者について成人身長が目標身長の-0.5SD以上を正常群,成人身長が目標身長の-0.5SD以下にとどまった群を低身長群としているが,低身長群は11名と半数であった。低身長群の危険因子を検討しているが発病年齢,月経開始年齢,発病身長と体重,罹病期間の最低体重に有意差を認めなかったが,$BMI<16\,kg/m^2$の期間が有意に低身長群で長期間(低身長群,24.9±3.2か月,正常群9.8±1.6か月)であったと報告している。やはり,やせの重症度がその後の成長に影響を与えていることを示唆している。堀川らは45名のANの患者で,8名が診断時以前より